

Protective Effects of Octyl Gallate Against Deoxynivalenol-Induced Colon Inflammation: Insights from Proteomic and Metabolomic Analyses

Chenxin Dongye, Xiangrong Chen,* Yanfang Zhao, Huijuan Li, Mohamed F. Abdallah, Tianliang Li, and Xiangfeng Chen*



Cite This: *Environ. Health* 2025, 3, 515–525

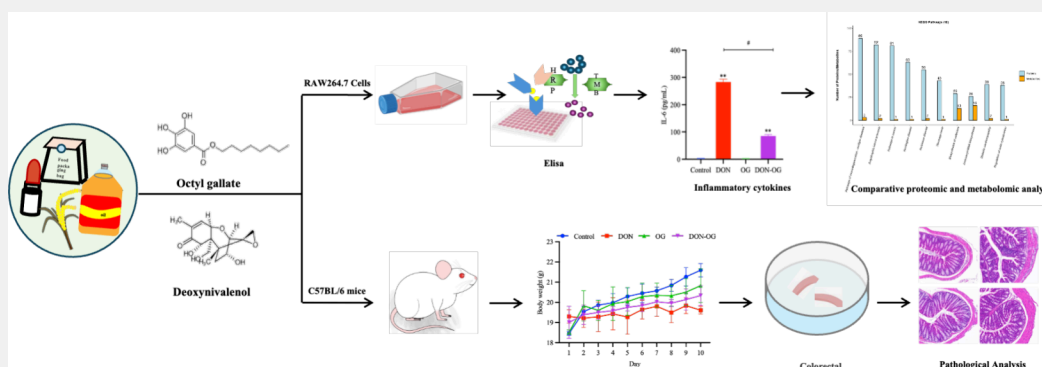


Read Online

ACCESS |

Metrics & More

Article Recommendations



ABSTRACT: Deoxynivalenol (DON) and octyl gallate (OG) are prevalent compounds in the environment and food. DON is frequently detected in cereals such as corn and wheat, while OG is commonly employed as a food additive. As a result, human exposure to these substances is inevitable. Given this, the objective of this experiment was to investigate the impact of co-exposure to DON (10 $\mu\text{g/kg}$) and OG (10 $\mu\text{g/kg}$) on intestinal inflammation. The RAW264.7 macrophage cell line was utilized to analyze cytokine levels as well as proteomic and metabolomic changes. In the quantitative real-time PCR experiments, the DON group showed significant difference compared to the control group (* $p < 0.05$) and the DON-OG group (# $p < 0.05$) regarding cytokine levels such as IL-10, TNF- α , IL6, IL1b, Ccl2, Il12 α , Nos2, Cxcl1, and Cxcl2. In the animal experiment, C57BL/6 mice were utilized to monitor body weight, the presence of bloody stools, and diarrhea. Additionally, the colonic tissues of the mice underwent pathological analysis. The results indicated that cells treated with both DON and OG displayed lower levels of inflammation compared to those treated with DON alone. Furthermore, proteomic and metabolomic analyses revealed that the regulation of the Lnc12 protein and the mTOR signaling pathway contributed to the milder inflammatory response observed in the DON-OG group. These findings were further corroborated by the pathological analysis of the colonic tissues from the mice. In the combined exposure of DON and OG, OG partially mitigated the intestinal inflammation induced by DON.

KEYWORDS: Octyl gallate, Deoxynivalenol, Inflammatory Bowel Disease, Metabolomics, Proteomics

INTRODUCTION

Currently, with the global environmental changes, such as climate change and land use change, the distribution and species of mycotoxins are also changing.^{1,2} Climate conditions (such as temperature and humidity) can directly affect fungal growth and toxin synthesis; for example, global warming may render may render certain areas more conducive to the growth of specific fungal toxins, thereby heightening the risk of crop contamination in these regions.³ Mycotoxins can cause damage to crops and feed, ultimately posing a threat to human health. Prolonged consumption of agricultural products contaminated with mycotoxins is harmful to humans.^{4,5} When crops contaminated with fungal toxins are used to produce feed

and then fed to poultry, livestock, fish, and other animals, fungal toxins can enter the human food chain and endanger human health.⁶ Additionally, mycotoxins are not only influenced by environmental factors but also can, in turn, affect the environment. For instance, they can contaminate

Received: November 24, 2024

Revised: January 24, 2025

Accepted: February 1, 2025

Published: February 6, 2025



ACS Publications

© 2025 The Authors. Co-published by Research Center for Eco-Environmental Sciences, Chinese Academy of Sciences, and American Chemical Society

Table 1. Sequences of Primers Used in RT-PCR

Gene	Forward primer sequence (5'–3')	Reverse primer sequence (5'–3')
Mouse <i>Il10</i>	CCCTTTGCTATGGTGTCTT	TGGTTTCTCTTCCCAAGACC
Mouse <i>Il12a</i>	GAGGACTTGAAGATGTACCAG	TCCTATCTGTGTGAGGAGGGC
Mouse <i>Cxcl1</i>	CTGGGATTACCTCAAGAAC	GAAGCCAGCGTTCACCAGAC
Mouse <i>Cxcl2</i>	AGTTTGCCTTGACCCTGAAGC	AGGCTCCTCCTTTCCAGG
Mouse <i>Nos2</i>	GCTCCTCGCTCAAGTTTCAGC	GTTTCTGGCAGCAGCGGCTC
Mouse <i>Il6</i>	AGCTGGAGTCACAGAAGGAG	AGGCATAACGCACTAGGTTT
Mouse <i>Tnfa</i>	GTCAGGTTGCCTCTGTCTCA	TCAGGGAAGAGTCTGGAAAG
Mouse <i>Ccl2</i>	CCACTCACCTGCTGCTACTCA	TGGTGATCCTCTTGCTAGCTCTCC
Mouse <i>Il1b</i>	GCAACTGTTCTGAACTCAACT	ATCTTTTGGGGTCCGTCAACT
Mouse <i>Actb</i>	AGGGCTATGCTCTCCCTCAC	CTCTCAGCTGTGGTGGTGAA

water sources and soil, thereby impacting the health of ecosystems.⁷ Among these mycotoxins, Deoxynivalenol (DON), also known as vomitoxin, is a common environmental toxin. It is a secondary metabolite produced by several *Fusarium* species and is widely present in cereals such as maize and wheat⁸ which is widely found in cereals such as maize and wheat.^{9,10} Due to its relatively stable chemical properties, resistance to heat and pressure, DON remains toxic for extended periods after contaminating food.^{11–13} This toxin can upregulate the production of inflammatory cytokines and chemokines, contributing to intestinal inflammation, which is characterized by symptoms like vomiting, weight loss, and diarrhea.^{14–17}

With the acceleration of modern life rhythms and the exacerbation of environmental pollution, environmental pollutants, such as airborne particulate matter, heavy metals, and other substances, can enter the human body through various channels. This leads to an increase in free radical production within the body, causing oxidative stress.¹⁸ Octyl gallate (OG), an ester derived from gallic acid, is a novel antioxidant widely used as a food additive.^{19,20} OG has demonstrated antimicrobial activity against *Helicobacter pylori*, enhances insulin secretion,²¹ and possesses antiviral and anti-inflammatory properties.¹⁹ Studies have shown that OG exerts anti-inflammatory effects in a rat model of endometriosis by inhibiting the nuclear factor- κ B (NF κ B) pathway.²² Moreover, OG can effectively exert its anti-inflammatory activity by directly binding to the NLRP3 LRR domain.²³ However, although there are some traditional toxicological studies on OG, existing research has shown that OG can disrupt mitochondrial function and inhibit caspase-3 related respiratory control.²⁴ Cordova et al. also confirmed that OG induces apoptotic cell death by activating caspase-3, leading to a loss of mitochondrial potential and mitochondrial dysfunction, accompanied by an increase in the expression of the pro-apoptotic protein Bax and the inhibition of the antiapoptotic protein Bcl-2.²⁵

Inflammatory bowel disease (IBD) is a general term for an idiopathic inflammatory change of the small intestine, colon, and rectum, encompassing conditions such as ulcerative colitis (UC) and Crohn's disease (CD).²⁶ The disease has the highest incidence in North America, Northern Europe, Western Europe, and Oceania. In North America, the incidence rate is approximately 20.2 cases per 100,000 people per year, and in Europe, it is about 3.22 cases per 100,000 people per year.²⁷ The etiology of IBD is complex and is generally associated with genetic and environmental factors, diet, smoking, and microbial infections.^{28–30} Inflammation plays a fundamental role in various physiological and pathological processes, significantly

influencing metabolism and neuroendocrine functions.^{31,32}

One of the hallmark of IBD is the elevated presence of inflammatory mediators.³³ These mediators, typically pro-inflammatory substances such as cytokines and chemokines, are closely correlated with the severity of inflammation.¹⁹ Cytokines, a class of proteins or small peptides that transmit signals between cells, possess immune regulatory and effector functions.³⁴ They are broadly classified into pro-inflammatory and anti-inflammatory cytokines, with their balance being critical to controlling inflammation.^{35,36}

DON is widely present in grains such as corn and wheat, while OG is used as a food additive and in food packaging materials.³⁷ Both compounds can easily and inevitably be ingested by humans or animals. Recent research has demonstrated the toxic effects of DON on humans and animals, with humans and pigs being the most sensitive.³⁸ Therefore, in this study, we explored the effects of DON-OG mixture exposure on intestinal inflammation and its mechanism of action at both cellular and animal levels through the metabolomics analysis, proteomics analysis, and pathological section of colorectal tissue.

MATERIALS AND METHODS

Chemical Reagents

The toxin deoxynivalenol (DON; CAS No. 51481–10–8, $\geq 98\%$ purity) was obtained from Macklin (Shanghai, China), while octyl gallate (OG; CAS No. 1034–01–1, 99.9% purity) was purchased from TMstandard (Beijing, China). DON and OG were dissolved in dimethyl sulfoxide acid (DMSO) at concentrations of 1 and 20 mg/mL, respectively, and stored at -20°C for later use. Fetal bovine serum (FBS) was supplied by ExCell Bio (FCS500, Shanghai, China). Dulbecco's modified eagle's medium (DMEM) with 4.5 g/L D-Glucose, L-Glutamine, 110 mg/L sodium pyruvate, penicillin/streptomycin antibiotics, nonessential amino acids (NEAA), and phosphate buffer saline (PBS) with and without Ca^{2+} and Mg^{2+} were all purchased from Gibco (Jinan, China).

Cell Culture Maintenance and Exposure to DON and OG

Mouse RAW 264.7 macrophage cell line was obtained from Procell (CL-0190, Wuhan, China) and cultured in DMEM medium supplemented with 10% FBS, penicillin/streptomycin (1%), and NEAA (1%) in a cell incubator at 37°C with 5% CO_2 . Cells were regularly subcultured when the confluency reached 80% of the cell culture flasks. For the experiment, RAW 264.7 cells were seeded in 96-well plates at a density of 2×10^5 cells/well and cultured in a cell incubator at 37°C , 5% CO_2 for 4 h. Next, the cells were treated with DON (0.01 $\mu\text{g/mL}$), OG (0.01 $\mu\text{g/mL}$) or a combination of DON (0.01 $\mu\text{g/mL}$) and OG (0.01 $\mu\text{g/mL}$) in the DON-OG treatment group.

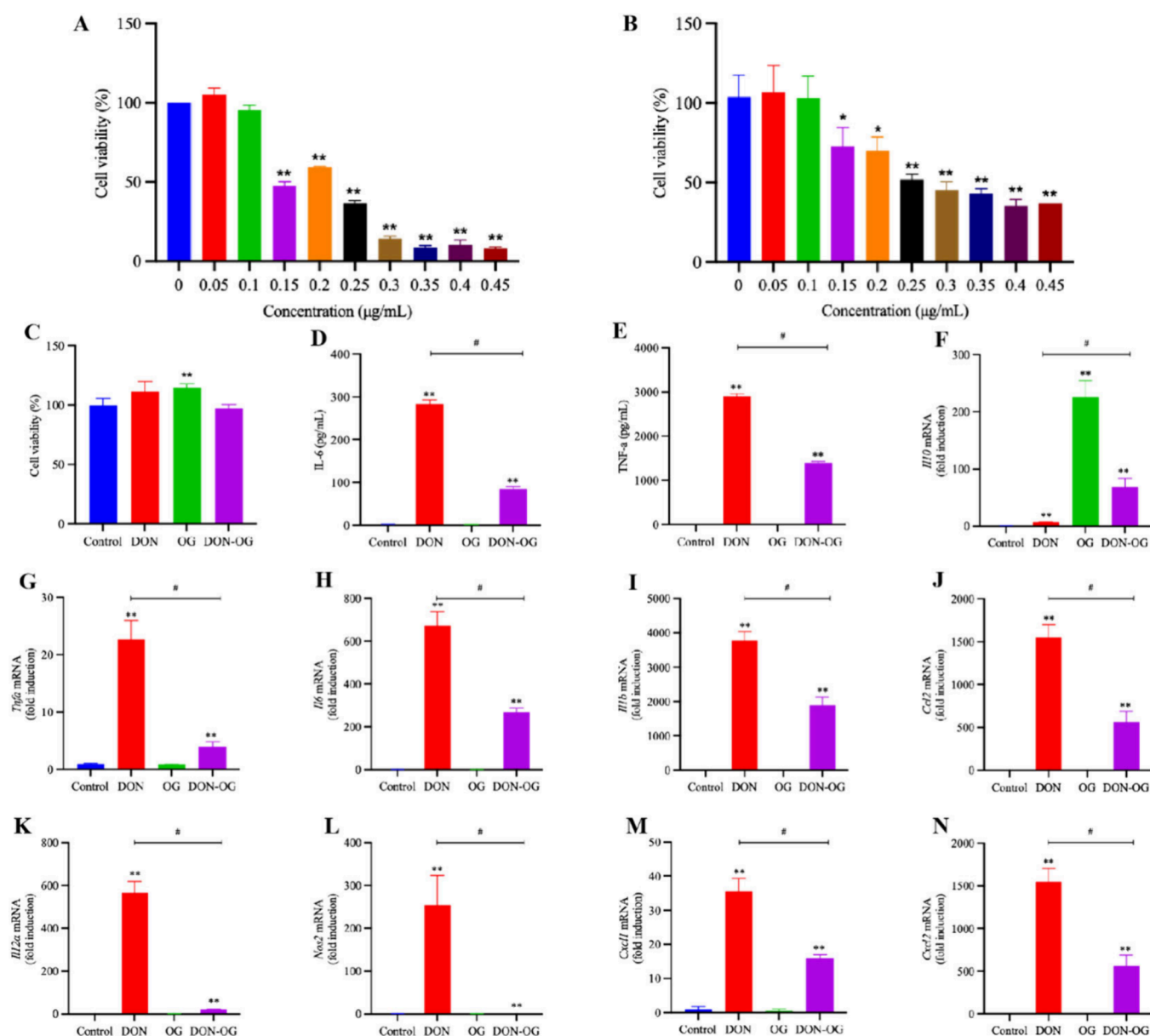


Figure 1. Cell viability at different concentrations of DON (A). Cell viability at different concentrations of OG (B). The cytotoxicity of DON (0.01 μg/mL), OG (0.01 μg/mL), DON-OG (0.01 μg/mL, 0.01 μg/mL) at the concentration used in the experiment (C). ELISA test for IL-6 (D). ELISA test for TNF-α (E). Quantitative real-time PCR for IL-10, TNF-α, IL6, IL1b, Ccl2, IL12α, Nos2, Cxcl1, Cxcl2 (F–N). Compared with control group, * $p < 0.05$, ** $p < 0.01$; compared with DON-OG group, # $p < 0.05$.

Cell Viability Assay

To evaluate cytotoxicity, a CCK-8 assay was performed using the Cell Counting Kit-8 (CCK-8; Nanjing Vazyme Biotech Co., Ltd., China) according to the manufacturer's instructions. Cultured cells were seeded into a 96-well plate and incubated at 37 °C with 5% CO₂ for 24 h with various concentrations or classes of compounds or left untreated as a control. Following treatment, 10 μL of a CCK-8 solution was added to each well. The plates were then incubated for an additional 4 h under the same conditions. Absorbance at 450 nm was measured by using a microplate reader to quantify cell viability.

Quantitative Real-Time Polymerase Chain Reaction (RT-PCR)

To assess cytokine expression at the mRNA level, quantitative reverse transcription PCR (RT-qPCR) was conducted. Total RNA was extracted using the Total RNA Isolation Reagent (Jinan, China). Complementary DNA (cDNA) was synthesized using Moloney murine leukemia virus reverse transcriptase (Invitrogen) at 38 °C for

60 min qPCR was performed on a LightCycler 480 II System (Roche) using an SYBR Green PCR Master Mix (Yeasen Biotechnology). Relative mRNA expression levels were calculated by using the $\Delta\Delta C_t$ method, with β -actin as the internal control. The sequences of forward and reverse primers used for qPCR are provided in Table 1.

ELISA for Expression of Cytokines

To evaluate cytokine levels in the cell supernatant, an enzyme-linked immunosorbent assay (ELISA) was performed. Supernatants from cultured cells were collected, and the concentrations of IL-6 and TNF-α were measured using ELISA kits (Jem-12, JEM-05; Anhui Joyee Biotechnics Co., Ltd., China).

LC-MS/MS based Metabolomics Analysis

To assess metabolite differences in the cell supernatants, untargeted metabolomics analysis was performed. Liquid nitrogen frozen samples were slowly thawed at 4 °C, and an appropriate volume of sample was mixed with a precooled methanol/acetonitrile/water solution (2:2:1, V/V) for metabolite extraction. The mixture was vortexed and

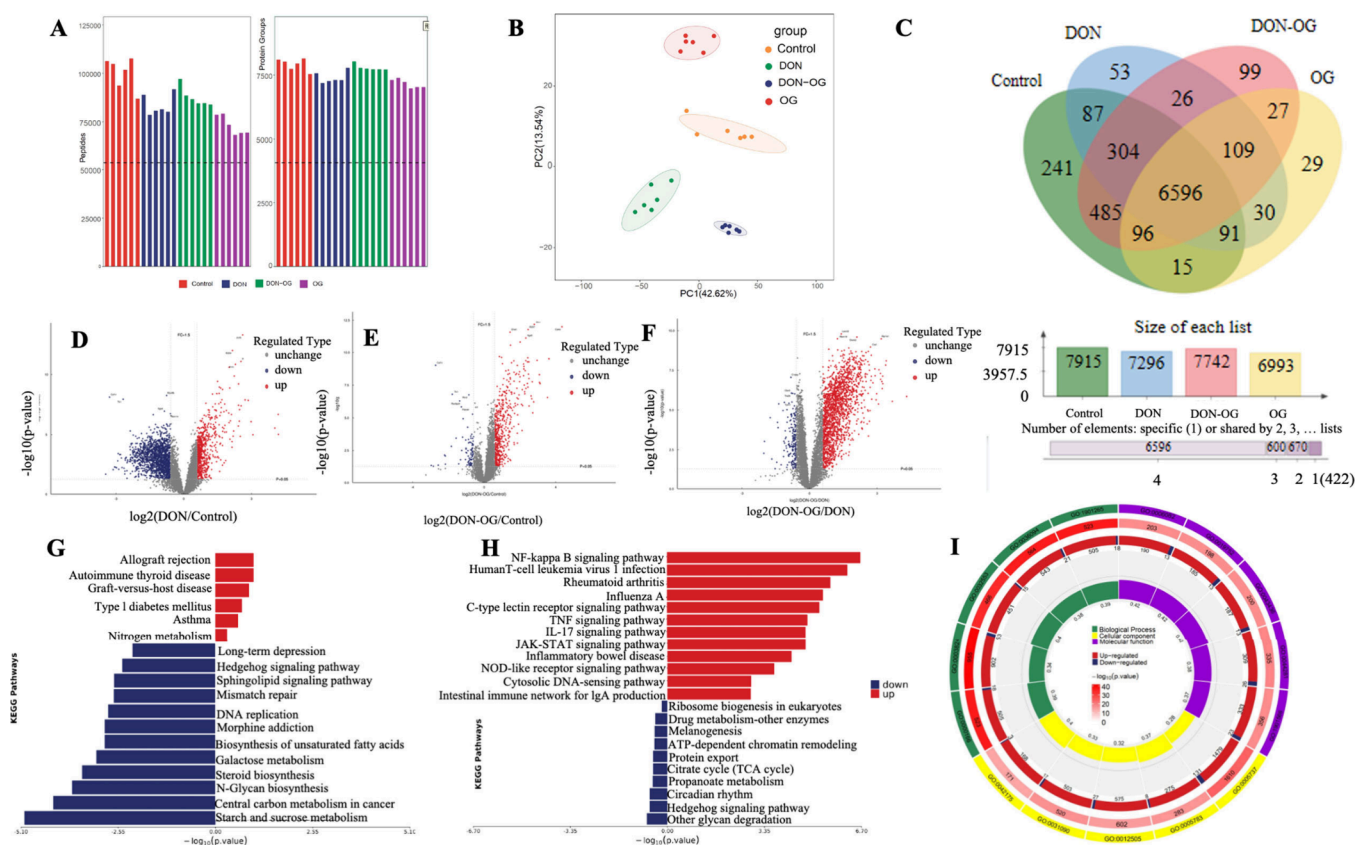


Figure 2. Proteomics analysis results. DIA identification results statistics bar chart (A). PCA distribution plot of all samples (B). Intergroup sample venn diagram (C). Volcano plot: DON vs control (D), DON-OG vs control (E), and DON-OG vs DON (F). Butterfly plot of pathway enrichment for significantly up and down regulated differentially expressed proteins: DON vs control (G) and DON-OG vs DON (H). Circos plot of GO enrichment for all differentially expressed proteins between the DON-OG group and DON group (I).

subjected to low-temperature ultrasound for 30 min, followed by incubation at -20°C for 10 min. Afterward, the samples were centrifuged at $14,000 \times g$ at 4°C for 20 min, and the supernatants were vacuum-dried. For the analysis, $100\ \mu\text{L}$ of 50% acetonitrile solution was added, and the samples were centrifuged at $14,000\ g$ at 4°C for 15 min. Metabolites were separated using an Agilent 1290 Infinity UHPLC system with a HILIC column, and mass spectrometric analysis was performed using an Orbitrap EXPLORER 480 mass spectrometer (Thermo Fisher). The positive and negative ion modes of electrospray ionization (ESI) were used for detection. ESI source and mass spectrum parameters were set as follows: atomizing gas auxiliary heating gas 1 (Gas1): 50, auxiliary heating gas 2 (Gas2): 2, ion source temperature: 350°C , spray voltage (ISVF) positive ion mode 3500 V, negative ion mode 2800 V; The first stage mass-to-charge ratio detection range: 70–1200 Da, resolution: 60000, scanning accumulation time: 100 ms; the second stage adopts segmented acquisition method, scanning range: 70–1200 Da, secondary resolution: 60000, scanning accumulation time: 100 ms, dynamic exclusion time: 4 s.

LC-MS/MS based Proteomics Analysis

To analyze proteins and peptides in the cell supernatant treated with different compounds, proteomics analysis was performed. Samples were analyzed using LC-MS/MS in DIA (data-independent acquisition) mode with an Astral Mass Spectrometer (Thermo Fisher). DIA analysis was performed on a Vanquish Neo system (Thermo Fisher Scientific) for chromatographic separation, and the separated samples were analyzed by DIA (data-independent acquisition) MS on a high-resolution Astral mass spectrometer (Thermo Scientific). The detection mode was positive ions with a scan range of 380–980 m/z , a first MS resolution of 240,000 at 200 m/z , a normalized AGC target of 500%, and a maximum IT of 5 ms.

MS2 was performed in DIA data acquisition mode with 299 scan windows set, an isolation window of 2 m/z , an HCD collision energy of 25 eV, a normalized AG target of 500%, and a maximum IT of 3 ms. Protein quantification was performed based on peptide analysis. Each sample was prepared independently, with protein extraction followed by enzymatic digestion to generate peptides for DIA analysis. The resulting DIA files were processed by using DIA-NN software for subsequent analysis. The mass spectrometry workflow included protein extraction, peptide enzymatic hydrolysis, LC-MS/MS DIA data collection, database searching, and both qualitative and quantitative analyses, followed by bioinformatics analysis.

Animal Experiments

To further evaluate the impact of the DON-OG mixture on animals, animal experiments were conducted using 60 male C57BL/6 mice (6–8 weeks old), purchased from Jinan Pengyue Experimental Animal Breeding Co., Ltd. (Jinan, China). All experiments were approved by the Animal Ethics Committee of Shandong Academy of Chinese Medicine (Animal Experiment Ethics Number: SDZYY20240116008) and were conducted in compliance with ethical guidelines for animal research. The mice were divided into four treatment groups with 15 mice per group and five mice per cage. The first group received intragastric administration of pure water for 5 days as a control. The second group was administered DON (10 $\mu\text{g}/\text{kg}$) intragastrically for 5 days, while the third group received OG (10 $\mu\text{g}/\text{kg}$) intragastrically for 5 days. The fourth group was treated with a combination of DON-OG (10 $\mu\text{g}/\text{kg}$ each) intrasternally for 5 days. After the treatment period, mice were euthanized on the eighth day, and the colonic-rectal length was measured. The colonic-rectal tissue was treated with normal saline (Servicebio, Wuhan, China, Cat: G4702–500 ML) and incubated in 1640 medium for 16 h.

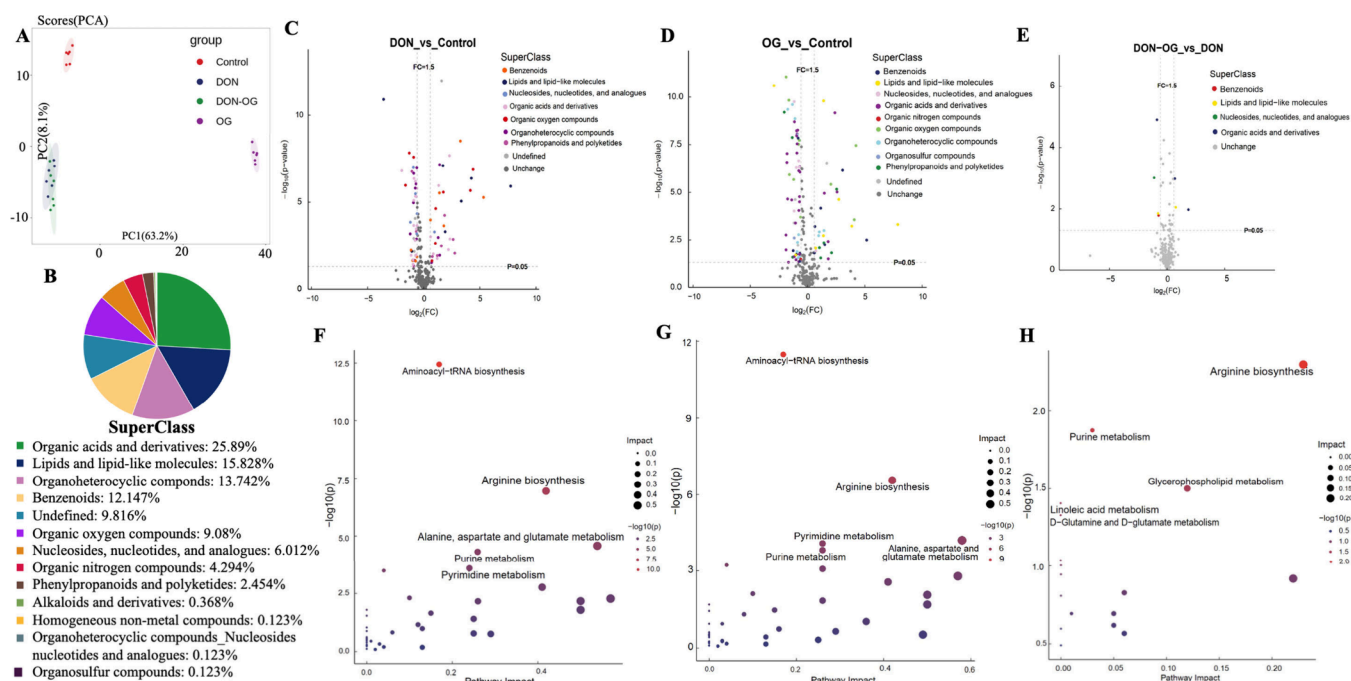


Figure 3. Metabolomics analysis results. Classification of identified metabolites (A). PCA Distribution Plot of All Samples (B). Volcano plot of material classification: DON vs control (C), DON-OG vs control (D), and DON-OG vs DON (E). KEGG enrichment bubble plot: DON vs control (F), OG vs control (G), and DON-OG vs DON (H).

Throughout the experiment, the weight changes, survival rate, bloody stool score, and diarrhea score were recorded daily until the 10th day.

Pathological Section of Colorectal Tissue

In order to visually observe the changes in the colorectal region of mice after treatment with different compounds, we conducted pathological section of colorectal tissue. After 5 days of continuous gavage, the mice in 4 groups were dissected on the eighth day, and their colons and rectum were washed with normal saline and put into 4% paraformaldehyde (Solarbio, Beijing, China). Hematoxylin and eosin (H&E) staining were performed by Qingdao Haosai Technology Co. LTD (Qingdao, China). Classical visual field images with SlideViewer were selected to be collected.

Statistical Analysis

All experiments were performed three times, and the mean values were taken for analysis. Statistical analysis was performed with SPSS 19.0 software (SPSS Inc., Chicago, IL). Statistical Evaluation of the data was performed using one-way analysis of variance when more than two groups were compared with a single control group and *t* test for differences between the two groups. Data are presented as the mean \pm standard deviation (SD). Compared with Control group, * *p* < 0.05, ** *p* < 0.01; compared with the mixture (DON-OG) group, # *p* < 0.05. Metabolomic and proteomic data analysis were mainly divided into student's *t* test, principal component analysis (PCA), boxplot analysis, cluster analysis, and KEGG analysis.

RESULTS

Cell Viability of DON, OG, and DON-OG Exposure in RAW264.7 Cells

As shown in Figure 1 (A,B), all tested concentrations reduced cell viability in a concentration-dependent manner. DON (0.01 μ g/mL), OG (0.01 μ g/mL), and DON-OG (0.01 μ g/mL, 0.01 μ g/mL) were selected, respectively, for cell activity testing. The results showed that as shown in Figure 1C, the experimental concentrations of the drug did not adversely affect cell activity compared with the control group.

Anti-inflammatory Effect of OG on DON of Inflammatory Cytokine

To understand the effect of OG on DON in RAW264.7 cells, RT-qPCR was used to detect the changes in inflammatory cytokines in the experimental group and the control group. As shown in Figure 1 (G-N), cells exposed to the DON group significantly upregulated expression levels of the pro-inflammatory cytokine (TNF- α , IL6, IL1b, Ccl2, IL12 α , Nos2, Cxcl1, Cxcl2). The expression level of anti-inflammatory cytokine (IL10) was significantly upregulated in OG-exposed cells. Cells exposed to DON-OG had significantly lower expression of proinflammatory cytokines (TNF- α , IL6, IL1b, Ccl2, IL12 α , Nos2, Cxcl1, Cxcl2) than cells exposed to DON, and the expression level of anti-inflammatory cytokine (IL10) was significantly higher than that of the cells exposed to DON.

Enzyme-Linked Immunosorbent Assay (ELISA) method was also used to detect the levels of cytokines in the supernatants of each group of cells. As shown in Figure 1 (D and E), compared with the control group, the pro-inflammatory cytokine (TNF- α , IL6) levels were significantly elevated in the DON group, and not significantly changed in the OG group, while the level of pro-inflammatory cytokines (TNF- α , IL6) increased significantly in the DON-OG group. Compared with the DON-OG group, the levels of pro-inflammatory cytokines (TNF- α , IL6) in the DON group were significantly increased.

Proteomics Analysis

In order to better understand the changes and mechanisms of the effects of DON-OG mixture exposure on inflammation, the DIA method was used to analyze the changes of cellular proteins. In total, more than 7,500 proteomes and more than 10,000 peptides were detected (Figure 2A). Of these, 53 proteins in the DON group differed from each other, 29 proteins in the OG group differed from each other, and 99 proteins in the DON-OG group differed from each other

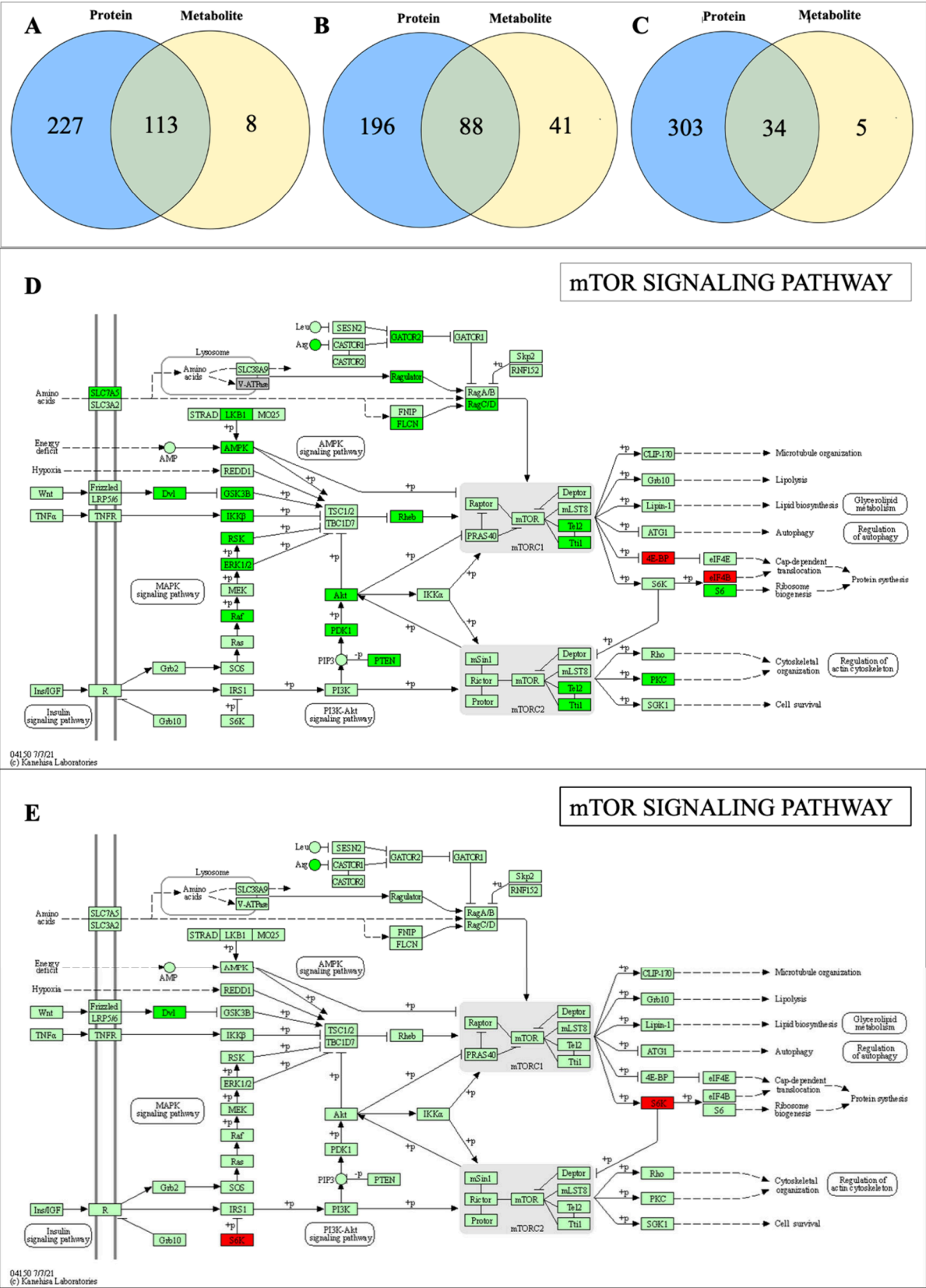


Figure 4. Proteomics and Nontargeted Metabolomics Combined with Bioinformatics Analysis. Venn diagram showing the pathways involved in the differentially expressed proteins and significantly different metabolites: DON vs control (A), DON-OG vs control (B), and DON-OG vs DON (C). Pathway map of differential proteins and significantly different metabolites: DON vs control (D) and DON-OG vs control (E).

(Figure 2C). As shown in Figure 2B, PCA indicates that the degree of clustering is high in each group, and the protein expression profiles of the samples are similar. The difference of protein between DON-OG group, DON group, OG group and

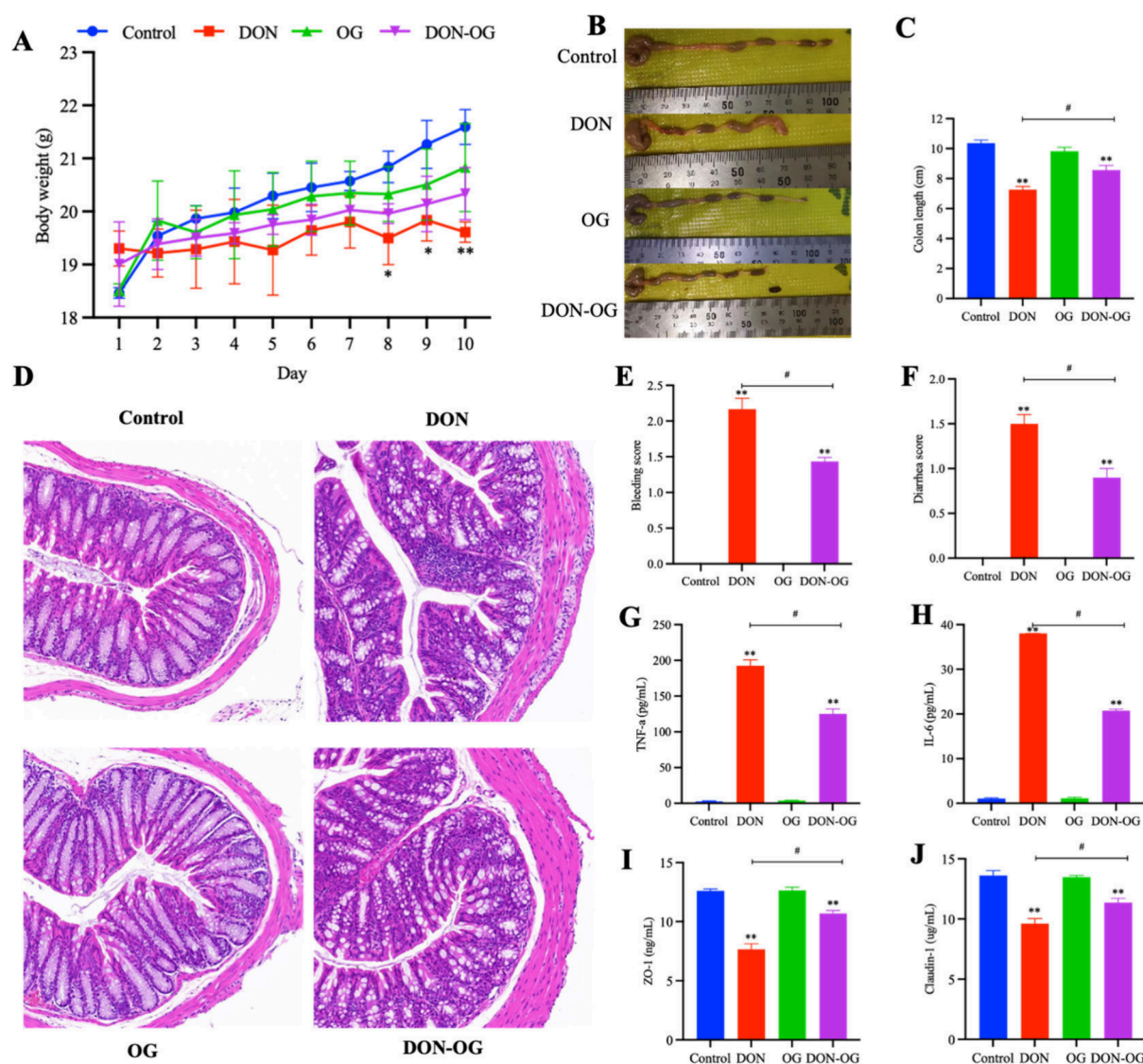


Figure 5. Animal experiment. Changes in mouse body weight (A). Changes in the length of the mouse colorectum (B) and (C). Pathological sections of mouse colorectal tissue (D). Bleeding score in mouse (E). Diarrhea score in mouse (F). ELISA test for TNF- α (G), IL-6 (H), ZO-1 (I) and claudin-1 (J). Compared with Control group, * $p < 0.05$, ** $p < 0.01$; compared with DON-OG group, # $p < 0.05$.

control group was obvious. As shown in the volcano plot (Figure 2D-F), the significantly downregulated proteins are labeled in blue ($FC < 0.67$ and $p < 0.05$), and the significantly upregulated proteins are labeled in red ($FC > 1.5$ and $p < 0.05$), the protein with no difference was gray, and the TOP 5 with the most significant difference in up-and down-regulated protein was labeled. As can be seen from Figure 2I, the number of proteins involved in biological processes, including nucleotide binding (GO: 0000166), catalytic activity (GO: 0003824), RNA modification (GO: 0032553), and small molecule binding (GO: 0036094) was significantly upregulated in the DON-OG group compared with the DON group. Additionally, the butterfly plot (Figure 2G and H) was constructed by using KEGG pathway enrichment analysis. Compared with the control group, the number of starch and sucrose metabolism, N-Glycan biosynthesis, central carbon metabolism in cancer, steroid biosynthesis and galactose metabolism proteins in DON group was significantly down-regulated. In the DON-OG group compared to the control

group, the number of proteins was downregulated in 8 pathways and significantly upregulated in 12 pathways.

Metabolomics Analysis

To further assess changes in metabolic pathways following DON-OG mixture exposure in RAW264.7 cells, UHPLC-Orbitrap Exploris480 MS were used to analyze changes in endogenous metabolites in both negative and positive ion modes. The identified compounds were categorized into 13 classes (Figure 3B). As shown in the PCA plot (Figure 3A), the DON-OG group, DON group, OG group, and the control group are relatively far apart, indicating significant metabolic differences between groups. Differential metabolites between different groups were classified by superclass (Figure 3C-E). As shown in the bubble plot by METPA enrichment analysis (Figure 3F-H), it is clearly observed that the levels of differential metabolites in Aminoacyl-tRNA biosynthesis, Arginine biosynthesis, Pyrimidine metabolism, and Alanine, aspartate, and glutamate metabolism were all high in the DON group vs control group and DON-OG group vs control group.

The level of Arginine biosynthesis in DON-OG group was significantly higher than that in DON group.

Combined Metabolomics and Proteomics Analysis

Through combined proteomic and metabolomic pathway analysis, it was discovered that there are 113 common pathways involving differentially expressed proteins (DEPs) and differentially accumulated metabolites (DAMs) between the DON group and the control group (Figure 4A). The number of pathways shared by DEPs and DAMs in the DON-OG group and the control group is 88 (Figure 4B), and the number of common pathways shared by DEPs and DAMs was 34 between the DON-OG group and DON group (Figure 4C). Of these, 4E-BP and eIF4B proteins were upregulated in the mTOR signaling pathway, 23 proteins were down-regulated, and the metabolite of Arg was downregulated (Figure 4D). In the DON-OG group, the protein of S6K was upregulated, the protein of Dvl downregulated, and a metabolite of Arg downregulated in the mTOR signaling pathway (Figure 4E).

Effects of OG and DON on Health and Body Weight in Mice

As shown in Figure 5A, the overall body weight of the mice tended to increase over 10 days, but that of the DON group was significantly lower than that of the control group. The DON-OG group grew more slowly than the control group and ended up weighing less, but the DON-OG group ended up weighing more than the DON group. The degree of bloody stools (Figure 5E) and diarrhea (Figure 5F) in mice was significantly more severe in the DON group and DON-OG group mice compared with the control group, and compared with the DON group, the conditions of mice bloody stools and diarrhea in the DON-OG group were milder. The mouse colorectal also can be observed (Figure 5B and C), which was significantly shorter in the DON group and the DON-OG group compared with the control group, and the colorectal length of DON-OG mice was longer than that of DON mice without significance. In addition, TNF- α (Figure 5G) and IL-6 (Figure 5H) levels were detected in the colorectum of mice in each group. Compared with the control group, the levels of TNF- α and IL-6 in DON group and DON-OG group were significantly higher, and the levels of TNF- α and IL-6 in DON group were also significantly higher than those in DON-OG group. The evaluation experiments of ZO-1 (Figure 5I) and claudin-1 (Figure 5J) tight junction proteins also showed that the levels of ZO-1 and claud-1 tight junction proteins in the DON group were significantly lower than those in the control group but the levels of tight junction proteins in the DON-OG group higher than those in the DON group, which was consistent with the results of the colorectal tissue pathological sections. By examining the pathological sections of colorectal tissues from mice (Figure 5D), it is found that the DON group exhibits loss of crypts, infiltration of inflammatory cells, increased distance between the crypt bases and the muscularis mucosa, and a decrease in the number of goblet cells compared with control group but not in OG group. The DON-OG group shows milder conditions compared to the DON group.

DISCUSSION

DON is considered a common and toxic mycotoxin in agricultural products,³⁹ and DON contamination is one of the challenging issues in food and feed safety fields.⁴⁰ At present, many studies are exploring how to prevent or alleviate the toxic

effects of DON on the human body. Additionally, studies have explored the effects of coexposure to DON-moniliformin (MON), DON-fumonisin B1 (FB1), DON-zearalenone (ZEA), and nivalenol (NIV)-T-2 toxin (T2) cell viability. These studies found that, after 48 h of exposure, the cell viability decreased in a dose-dependent manner for the most cytotoxic mycotoxin T2. Regarding the mycotoxin mixtures, they mainly exhibited antagonistic effects on cell viability reduction.⁴¹ There some research has shown that DON inhibits cell proliferation in the thymus of mice and affects biological processes, including ribosome and mitochondria function, T lymph activation, and cell apoptosis.⁴² RAW 264.7 macrophage line was selected as an inflammatory cell culture model, which widely used in the research of inflammation, immunity, apoptosis, tumor and other fields, especially in the study of inflammation, as a common in vitro model for screening anti-inflammatory agents and studying inflammatory mechanisms.⁴³ The study on the impact of DON exposure time and dose on Hepa 1–6 cell viability found that cell viability is time-dependent at low doses long-term exposure.⁴⁴ And in experimental animal models, acute DON poisoning leads to vomiting, while chronic low-dose exposure causes anorexia, growth retardation, immunotoxicity and reproductive and developmental damage due to maternal toxicity.⁴⁵ Considering the fast growth rate of RAW264.7 cells, we opted for high-dose, short-term exposure. In the study, we investigated the effects of the combination of DON and OG on the Lancl2 protein and the mTOR signaling pathway. The study demonstrated at both the cellular and mouse levels that the combination of DON and OG can partially inhibit the inflammation caused by DON.

Lancl2 protein, also known as lanthionine synthetase C-like protein 2, is an abscis acid receptor expressed in human immune cells, epithelial cells, and muscle cells, participating in signal transduction related to stress response, tissue growth, inflammation regulation, glucose metabolism.^{46–48} The activation of the Lancl2 pathway has been shown to be beneficial for various autoimmune, inflammatory, and metabolic conditions, including IBD.⁴⁹ The Lancl2 in phagocytes impairs phagosome processing, leading to increased uptake of materials and production of inflammatory cytokines.⁵⁰ The mechanism by which improves IBD may involve activating the Lancl2 pathway to regulate the production of pro-inflammatory cytokines, proliferation, and glucose metabolism.^{50–52} It may also support the of regulatory T cells through immunometabolic mechanisms, thereby improving IBD.⁵² Specifically, it may help to suppress the inflammatory response in IBD. Research conducted both in vivo and in vitro in mice has shown that Lancl2 gene knockout mice exhibit increased disease activity, weight loss, and enhanced severity of colonic inflammatory lesions. This indicates a close relationship between Lancl2 protein and inflammation, and it is possible that it exerts this anti-inflammatory effect through its signaling pathway.⁵² The DON-OG group showed a significant upregulation of Lancl2 protein compared to that of the DON group (Figure 2F), indicating that the combined exposure of DON-OG reduces intestinal inflammation more than the exposure to DON alone.

The mammalian target of rapamycin (mTOR) is a master regulator of many critical cellular activities, playing a significant role in various physiological processes, such as cell growth, metabolism, angiogenesis homeostasis, autophagy, and senescence. It is also associated with the occurrence of various

diseases and tumor resistance.^{53,54} Moreover, mTOR plays a crucial role in inflammation-related diseases, influencing inflammatory responses in multiple ways. For instance, the mTOR pathway can regulate the production of cytokines, affect function of immune cells, and participate in the release of inflammatory mediators.⁵⁵ In certain cases, the overactivation of the mTOR pathway may lead to a chronic inflammation state, which could be related to the pathogenesis of various inflammation-related diseases.⁵⁵ Many studies have shown that the activated mTOR pathway promotes the development of IBD. Additionally, research using mTOR inhibitors in mouse models of IBD has found that targeting mTOR can not only prevent colitis but also further inhibit the development of colon cancer in patients with inflammatory bowel disease.^{56,57} In the DON group compared to the control group (Figure 4D) and the DON-OG group compared to the control group (Figure 4F), the LKB1 and AMPK proteins in the mTOR pathway were significantly downregulated, which represents the mixture of DON and OG has been shown to mitigate intestinal inflammation more effectively than DON alone.

LKB1 can indirectly negatively regulate the mTOR signaling pathway by activating AMPK, and it can also directly negatively regulate the mTOR signaling pathway. Specifically, LKB1 directly phosphorylates the Raptor subunit of mTORC1, thereby inhibiting the role of mTORC1 in promoting cell growth metabolism.^{58–60} Additionally, LKB1 can promote the formation of the TSC1/TSC2 complex, which acts as a negative regulator of mTORC1.⁶¹ Therefore, the solitary toxin effect activates the mTOR signaling pathway by down-regulating the LKB1 protein, thereby promoting IBD.

AMPK is a protein kinase that senses the energy state of the cell, being activated when cellular ATP levels decrease or the AMP/ATP ratio increases. Activated AMPK can inhibit cell growth and proliferation by suppressing the mTORC1 signaling pathway.^{62–64} In contrast, the significant down-regulation of AMPK in Figure 4D compared with Figure 4F indicates that the mTOR signaling pathway was not inhibited, thereby promoting IBD.

Acute enteritis may lead to a transient increase in uric acid excretion, causing an elevation in blood uric acid concentration.⁶⁵ On the other hand, chronic intestinal inflammation may lead to abnormal uric acid metabolism, which can also cause an increase in uric acid levels.⁶⁵ Our study found that compared to the DON-OG group, the metabolite uric acid levels were higher in the DON group, indicating that the group exposed solely to DON had a more pronounced trend of IBD than the group exposed to the DON-OG mixture.

CONCLUSION

In conclusion, the obtained data demonstrate that DON and DON-OG can affect IBD levels through the Lnc2 protein and the mTOR pathway. Notably mixed exposure to DON-OG can partially alleviate the increase in IBD levels caused by DON. And it can partially alleviate the intestinal inflammation caused by DON by suppressing pro-inflammatory cytokines, regulatory proteins, and inflammatory pathways. However, the common effects and mechanisms of action of different toxins and different antioxidants may not be the same, including fusarium toxins and synthetic phenol antioxidants (new pollution in the environment). In particular, the issue of potential coexposure to enhanced toxicity needs to be addressed, and more work will be needed in the future, such

as animal pathology studies and metabolic transformation studies of compounds.

AUTHOR INFORMATION

Corresponding Authors

Xiangrong Chen — Shandong International Joint Laboratory of Environmental and Biological Science, Qilu University of Technology (Shandong Academy of Science), Jinan, Shandong 250014, China; Email: xiangfchensdas@163.com

Xiangfeng Chen — Shandong International Joint Laboratory of Environmental and Biological Science, Qilu University of Technology (Shandong Academy of Science), Jinan, Shandong 250014, China; orcid.org/0000-0001-9056-7585; Email: xrchen0719@outlook.com

Authors

Chenxin Dongye — Shandong International Joint Laboratory of Environmental and Biological Science, Qilu University of Technology (Shandong Academy of Science), Jinan, Shandong 250014, China

Yanfeng Zhao — Shandong International Joint Laboratory of Environmental and Biological Science, Qilu University of Technology (Shandong Academy of Science), Jinan, Shandong 250014, China

Huijuan Li — Shandong International Joint Laboratory of Environmental and Biological Science, Qilu University of Technology (Shandong Academy of Science), Jinan, Shandong 250014, China

Mohamed F. Abdallah — Department of Human Biology and Toxicology, Faculty of Medicine, Pharmacy and Biomedical Sciences, University of Mons, Mons 7000, Belgium; orcid.org/0000-0002-3903-6452

Tianliang Li — Center for Cell Structure and Function, Shandong Provincial Key Laboratory of Animal Resistance Biology, Collaborative Innovation Center of Cell Biology in Universities of Shandong, College of Life Sciences, Shandong Normal University, Jinan 250358, China

Complete contact information is available at:

<https://pubs.acs.org/10.1021/envhealth.4c00250>

Notes

The authors declare no competing financial interest.

ACKNOWLEDGMENTS

This work was supported by the National Natural Science Foundation of China (No. 22074071), Key Research and Development Program of Shandong Province (2024KJHZ032), the Program for Taishan Scholars of Shandong Province (NO. tsqn 202103099, X. Chen) and the Pilot Project on the Integration of Science Education and Production of Qilu University of Technology (2024GH23).

REFERENCES

- (1) Juraschek, L. M.; Kappenberg, A.; Amelung, W. Mycotoxins in soil and environment. *Science of The Total Environment* **2022**, 814, No. 152425.
- (2) Alam, S.; Nisa, S.; Daud, S.; Mycotoxins in environment and its health implications. In *Hazardous Environmental Micro-pollutants, Health Impacts and Allied Treatment Technologies*. Springer International Publishing, 2022, 289–318.

- (3) Marroquín-Cardona, A. G.; Johnson, N. M.; Phillips, T. D.; Hayes, A. W. Mycotoxins in a changing global environment—a review. *Food Chem. Toxicol.* **2014**, *69*, 220–230.
- (4) Nestic, K.; Ivanovic, S.; Nestic, V. Fusarial toxins: secondary metabolites of *Fusarium* fungi. *Reviews of Environmental Contamination and Toxicology* **2014**, *228*, 101–120.
- (5) Guo, H.; Ji, J.; Wang, J.; Sun, X. Co-contamination and interaction of fungal toxins and other environmental toxins. *Trends in Food Science & Technology* **2020**, *103*, 162–178.
- (6) Xu, J. Assessing global fungal threats to humans. *mLife* **2022**, *1* (3), 223–240.
- (7) Singh, V. K.; Meena, M.; Zehra, A.; Tiwari, A.; Dubey, M. K.; Upadhyay, R. S. Fungal toxins and their impact on living systems. *Microbial diversity and biotechnology in food security* **2014**, 513–530.
- (8) Pestka, J. J.; Smolinski, A. T. Deoxynivalenol: toxicology and potential effects on humans. *Journal of Toxicology and Environmental Health-Part B-Critical Reviews* **2005**, *8* (1), 39–69.
- (9) European Food Safety Authority. Deoxynivalenol in food and feed: Occurrence and exposure. *EFSA Journal* **2013**, *11* (10), 3379.
- (10) Ji, X.; Yang, H.; Wang, J.; Li, R.; Zhao, H.; Xu, J.; Xiao, Y.; Tang, B.; Qian, M. Occurrence of deoxynivalenol (DON) in cereal-based food products marketed through e-commerce stores and an assessment of dietary exposure of Chinese consumers to DON. *Food Control* **2018**, *92*, 391–398.
- (11) Xu, L.; Liu, Y.; Pei, Y.; Wen, Y.; Ma, Y. Determination of deoxynivalenol in corn oil by HPLC with multifunctional purification column. *CABI Databases* **2016**, 83–86.
- (12) Cao, H.; Wu, S.; Sun, C. Research advancement on biosynthesis and biodegradation of Deoxynivalenol (DON). *Journal of the Chinese Cereals and Oils Association* **2013**, *28*, 116–123.
- (13) Yao, Y.; Long, M. The biological detoxification of deoxynivalenol: A review. *Food Chem. Toxicol.* **2020**, *145*, No. 111649.
- (14) Hooft, J. M.; Bureau, D. P. Deoxynivalenol: Mechanisms of action and its effects on various terrestrial and aquatic species. *Food Chem. Toxicol.* **2021**, *157*, No. 112616.
- (15) Tominaga, M.; Momonaka, Y.; Yokose, C.; Tadaishi, M.; Shimizu, M.; Yamane, T.; Oishi, Y.; Kobayashi-Hattori, K. Anorexic action of deoxynivalenol in hypothalamus and intestine. *Toxicol.* **2016**, *118*, 54–60.
- (16) Bonnet, M. S.; Roux, J.; Mounien, L.; Dallaporta, M.; Troadec, J. D. Advances in deoxynivalenol toxicity mechanisms: the brain as a target. *Toxins* **2012**, *4* (11), 1120–1138.
- (17) Pestka, J. J. Deoxynivalenol: mechanisms of action, human exposure, and toxicological relevance. *Arch. Toxicol.* **2010**, *84*, 663–679.
- (18) Mudway, I. S.; Kelly, F. J.; Holgate, S. T. Oxidative stress in air pollution research. *Free Radical Biol. Med.* **2020**, *151*, 2.
- (19) Haute, G. V.; Luft, C.; Antunes, G. L.; Silveira, J. S.; de Souza Basso, B.; da Costa, M. S.; Levorse, V. G. S.; Kaiber, D. B.; Donadio, M. V. F.; Gracia Sancho, J.; de Oliveira, J. R. Anti-inflammatory effect of octyl gallate in alveolar macrophages cells and mice with acute lung injury. *Journal of Cellular Physiology* **2020**, *235* (9), 6073–6084.
- (20) Yang, J.; Gould, T. J.; Jeon, B.; Ji, Y. Broad-Spectrum Antibacterial Activity of Antioxidant Octyl Gallate and Its Impact on Gut Microbiome. *Antibiotics* **2024**, *13* (8), 731.
- (21) Latha, R. C. R.; Daisy, P. Therapeutic potential of octyl gallate isolated from fruits of *Terminalia bellerica* in streptozotocin-induced diabetic rats. *Pharmaceutical Biology* **2013**, *51* (6), 798–805.
- (22) Bustami, A.; Hayuningrum, C. F.; Lestari, W. P.; Wibowo, H.; Wuyung, P. E.; Natadisastra, R. M. The anti-inflammatory effect of octyl gallate through inhibition of nuclear factor- κ B (NF- κ B) pathway in rat endometriosis model. *Journal of Reproduction and Fertility* **2021**, *21* (3), 169.
- (23) Park, H.; Ko, R.; Seo, J.; Ahn, G. Y.; Choi, S. W.; Kwon, M.; Lee, S. Y. Octyl gallate has potent anti-inflammasome activity by directly binding to NLRP3 LRR domain. *Journal of Cellular Physiology* **2024**, *239* (4), No. e31196.
- (24) Nakagawa, Y.; Tayama, S. Cytotoxicity of propyl gallate and related compounds in rat hepatocytes. *Arch. Toxicol.* **1995**, *69*, 204–208.
- (25) Cordova, C. A. S. d.; Locatelli, C.; Assuncao, L. S.; Mattei, B.; Mascarello, A.; Winter, E.; Nunes, R. J.; Yunes, R. A.; Creczynski-Pasa, T. B. Octyl and dodecyl gallates induce oxidative stress and apoptosis in a melanoma cell line. *Toxicology in Vitro* **2011**, *25* (8), 2025–2034.
- (26) de Mattos, B. R. R.; Garcia, M. P. G.; Nogueira, J. B.; Paiatto, L. N.; Albuquerque, C. G.; Souza, C. L.; Fernandes, L. G. R.; Tamashiro, W. M. d. S. C.; Simioni, P. U. Inflammatory bowel disease: an overview of immune mechanisms and biological treatments. *Mediators of Inflammation* **2015**, *2015* (1), No. 493012.
- (27) Ng, S. C.; Shi, H. Y.; Hamidi, N.; Underwood, F. E.; Tang, W.; Benchimol, E. I.; Panaccione, R.; Ghosh, S.; Wu, J. C. Y.; Chan, F. K. L.; Sung, J. J. Y.; Kaplan, G. G. Worldwide incidence and prevalence of inflammatory bowel disease in the 21st century: a systematic review of population-based studies. *Lancet* **2017**, *390* (10114), 2769–2778.
- (28) Carbonnel, F.; Jantchou, P.; Monnet, E.; Cosnes, J. Environmental risk factors in Crohn's disease and ulcerative colitis: an update. *Gastroenterology and Clinical Biology* **2009**, *33*, S145–S157.
- (29) Ng, S. C.; Bernstein, C. N.; Vatn, M. H.; Lakatos, P. L.; Loftus, E. V.; Tysk, C.; O'Morain, C.; Moum, B.; Colombel, J.-F. Geographical variability and environmental risk factors in inflammatory bowel disease. *Gut* **2013**, *62* (4), 630–649.
- (30) Agrawal, M.; Allin, K. H.; Petralia, F.; Colombel, J. F.; Jess, T. Multiomics to elucidate inflammatory bowel disease risk factors and pathways. *Nature Reviews Gastroenterology & Hepatology* **2022**, *19* (6), 399–409.
- (31) Zhang, W.; Lin, H.; Zou, M.; Yuan, Q.; Huang, Z.; Pan, X.; Zhang, W. Nicotine in inflammatory diseases: anti-inflammatory and pro-inflammatory effects. *Frontiers in Immunology* **2022**, *13*, No. 826889.
- (32) Varela, M. L.; Mogildea, M.; Moreno, I.; Lopes, A. Acute inflammation and metabolism. *Inflammation* **2018**, *41*, 1115–1127.
- (33) Chougule, P. R.; Sangaraju, R.; Patil, P. B.; Qadri, S. S. Y. H.; Panpatil, V. V.; Ghosh, S.; Mungamuri, S. K.; Bhanoori, M.; Sinha, S. N. Effect of ethyl gallate and propyl gallate on dextran sulfate sodium (DSS)-induced ulcerative colitis in C57BL/6 J mice: preventive and protective. *Inflammopharmacology* **2023**, *31* (4), 2103–2120.
- (34) O'Shea, J. J.; Gadina, M.; Siegel, R. M. Cytokines and cytokine receptors. *Clinical Immunology* **2019**, 127–155.
- (35) Whicher, J. T.; Evans, S. W. Cytokines in disease. *Clinical Chemistry* **1990**, *36* (7), 1269–1281.
- (36) Tayal, V.; Kalra, B. S. Cytokines and anti-cytokines as therapeutics—An update. *Eur. J. Pharmacol.* **2008**, *579* (1–3), 1–12.
- (37) Salavati Hamedani, M.; Rezaeigolestani, M.; Mohsenzadeh, M. Optimization of antibacterial, physical and mechanical properties of novel chitosan/olibanum gum film for food packaging application. *Polymers* **2022**, *14* (19), 3960.
- (38) Sun, Y.; Jiang, J.; Mu, P.; Lin, R.; Wen, J.; Deng, Y. Toxicokinetics and metabolism of deoxynivalenol in animals and human. *Arch. Toxicol.* **2022**, *96* (10), 2639–2654.
- (39) Takemura, H.; Shim, J. Y.; Sayama, K.; Tsubura, A.; Zhu, B. T.; Shimoi, K. Characterization of the estrogenic activities of zearalenone and zeranol in vivo and in vitro. *Journal of Steroid Biochemistry and Molecular Biology* **2007**, *103* (2), 170–177.
- (40) Sobrova, P.; Adam, V.; Vasatkova, A.; Beklova, M.; Zeman, L.; Kizek, R. Deoxynivalenol and its toxicity. *Interdisciplinary Toxicology* **2010**, *3* (3), 94–99.
- (41) Smith, M.-C.; Madec, S.; Troadec, S.; Coton, E.; Hymery, N. Effects of fusariotoxin co-exposure on THP-1 human immune cells. *Cell Biology and Toxicology* **2018**, *34*, 191–205.
- (42) Katika, M. R.; Hendriksen, P. J. M.; van Loveren, H. Characterization of the modes of action of deoxynivalenol (DON) in the human Jurkat T-cell line. *Journal of Immunotoxicology* **2015**, *12* (3), 206–216.

- (43) Kong, L.; Smith, W.; Hao, D. Overview of RAW264. 7 for osteoclastogenesis study: Phenotype and stimuli. *Journal of Cellular and Molecular Medicine* **2019**, *23* (5), 3077–3087.
- (44) Pierron, A.; Mimoun, S.; Murate, L. S.; Loiseau, N.; Lippi, Y.; Bracarense, A.-P. F. L.; Schatzmayr, G.; He, J. W.; Zhou, T.; Moll, W.-D.; Oswald, I. P. Microbial biotransformation of DON: molecular basis for reduced toxicity. *Sci. Rep.* **2016**, *6* (1), 29105.
- (45) Pestka, J. J. Deoxynivalenol: mechanisms of action, human exposure, and toxicological relevance. *Arch. Toxicol.* **2010**, *84*, 663–679.
- (46) Fresia, C.; Vigliarolo, T.; Guida, L.; Booz, V.; Bruzzone, S.; Sturla, L.; Di Bona, M.; Pesce, M.; Usai, C.; De Flora, A.; Zocchi, E. G-protein coupling and nuclear translocation of the human abscisic acid receptor LANCL2. *Sci. Rep.* **2016**, *6* (1), 26658.
- (47) Zeng, M.; Van Der Donk, W. A.; Chen, J. Lanthionine synthetase C-like protein 2 (LanCL2) is a novel regulator of Akt. *Molecular Biology of The Cell* **2014**, *25* (24), 3954–3961.
- (48) Sturla, L.; Fresia, C.; Guida, L.; Bruzzone, S.; Scarfi, S.; Usai, C.; Zocchi, E. LANCL2 is necessary for abscisic acid binding and signaling in human granulocytes and in rat insulinoma cells. *J. Biol. Chem.* **2009**, *284* (41), 28045–28057.
- (49) Tubau-Juni, N.; Hontecillas, R.; Leber, A. J.; Alva, S. S.; Bassaganya-Riera, J. Treating Autoimmune Diseases With LANCL2 Therapeutics: A Novel Immunoregulatory Mechanism for Patients With Ulcerative Colitis and Crohn's Disease. *Inflammatory Bowel Diseases* **2024**, *30* (4), 671–680.
- (50) Leber, A.; Bassaganya-Riera, J.; Tubau-Juni, N.; Zoccoli-Rodriguez, V.; Viladomiu, M.; Abedi, V.; Lu, P.; Hontecillas, R. Modeling the role of lanthionine synthetase C-like 2 (LANCL2) in the modulation of immune responses to helicobacter pylori infection. *PLoS One* **2016**, *11* (12), No. e0167440.
- (51) Tubau-Juni, N.; Hontecillas, R.; Leber, A.; Maturavongsadit, P.; Chauhan, J.; Bassaganya-Riera, J. First-in-class topical therapeutic omilancor ameliorates disease severity and inflammation through activation of LANCL2 pathway in psoriasis. *Sci. Rep.* **2021**, *11* (1), 19827.
- (52) Leber, A.; Hontecillas, R.; Zoccoli-Rodriguez, V.; Bassaganya-Riera, J. Activation of LANCL2 by BT-11 ameliorates IBD by supporting regulatory T cell stability through immunometabolic mechanisms. *Inflammatory Bowel Diseases* **2018**, *24* (9), 1978–1991.
- (53) Laplante, M.; Sabatini, D. M. mTOR signaling in growth control and disease. *Cell* **2012**, *149* (2), 274–293.
- (54) Zou, Z.; Tao, T.; Li, H.; Zhu, X. mTOR signaling pathway and mTOR inhibitors in cancer: progress and challenges. *Cell & Bioscience* **2020**, *10* (1), 31.
- (55) Weichhart, T.; Säemann, M. D. The PI3K/Akt/mTOR pathway in innate immune cells: emerging therapeutic applications. *Annals of the Rheumatic Diseases* **2008**, *67*, iii70–iii74.
- (56) Bhonde, M. R.; Gupte, R. D.; Dadarkar, S. D.; Jadhav, M. G.; Tannu, A. A.; Bhatt, P.; Dagia, N. M. A novel mTOR inhibitor is efficacious in a murine model of colitis. *American Journal of Physiology-Gastrointestinal and Liver Physiology* **2008**, *295* (6), G1237–G1245.
- (57) Zhang, Z.; Dong, L.; Jia, A.; Chen, X.; Yang, Q.; Wang, Y.; Liu, G. Glucocorticoids promote the onset of acute experimental colitis and cancer by upregulating mTOR signaling in intestinal epithelial cells. *Cancers* **2020**, *12* (4), 945.
- (58) Gwinn, D. M.; Shackelford, D. B.; Egan, D. F.; Mihaylova, M. M.; Mery, A.; Vasquez, D. S.; Turk, B. E.; Shaw, R. J. AMPK phosphorylation of raptor mediates a metabolic checkpoint. *Mol. Cell* **2008**, *30* (2), 214–226.
- (59) Shaw, R. J. LKB1 and AMP-activated protein kinase control of mTOR signalling and growth. *Acta Physiologica* **2009**, *196* (1), 65–80.
- (60) Green, A. S.; Chapuis, N.; Lacombe, C.; Mayeux, P.; Bouscary, D.; Tamburini, J. LKB1/AMPK/mTOR signaling pathway in hematological malignancies: from metabolism to cancer cell biology. *Cell Cycle* **2011**, *10* (13), 2115–2120.
- (61) van Veelen, W.; Korsse, S. E.; van de Laar, L.; Peppelenbosch, M. P. The long and winding road to rational treatment of cancer associated with LKB1/AMPK/TSC/mTORC1 signaling. *Oncogene* **2011**, *30* (20), 2289–2303.
- (62) Hahn-Windgassen, A.; Nogueira, V.; Chen, C. C.; Skeen, J. E.; Sonenberg, N.; Hay, N. Akt activates the mammalian target of rapamycin by regulating cellular ATP level and AMPK activity. *J. Biol. Chem.* **2005**, *280* (37), 32081–32089.
- (63) Kimura, N.; Tokunaga, C.; Dalal, S.; Richardson, C.; Yoshino, K. I.; Hara, K.; Kemp, B. E.; Witters, L. A.; Mimura, O.; Yonezawa, K. A possible linkage between AMP-activated protein kinase (AMPK) and mammalian target of rapamycin (mTOR) signalling pathway. *Genes Cells* **2003**, *8* (1), 65–79.
- (64) Xu, J.; Ji, J.; Yan, X. H. Cross-talk between AMPK and mTOR in regulating energy balance. *Critical Reviews in Food Science and Nutrition* **2012**, *52* (5), 373–381.
- (65) Zhu, F.; Feng, D.; Zhang, T. Altered uric acid metabolism in isolated colonic Crohn's disease but not ulcerative colitis. *Journal of Gastroenterology and Hepatology* **2019**, *34* (1), 154–161.